A Case Modeling of Sea–Land Breeze in Macao and Its Neighborhood①

Lin Wenshi(林文实), Wang Anyu(王安宇) and Wu Chisheng(吴池胜)

Department of Atmospheric Sciences, Zhongshan University, Guangzhou 510275

Fong Soi Kun(冯瑞权)

Macao Meteorological and Geophysical Bureau, Macao

Department of Atmospheric Sciences, Zhongshan University, Guangzhou 510275

Ku Chimeng(古志明)

Macao Meteorological and Geophysical Bureau, Macao

(Received August 29, 2000; revised October 26, 2000)

ABSTRACT

PSU / NCAR MM5 was utilized to simulate the sea–land breeze circulation in Macao and the three–dimensional flow around the Pearl River estuary. Four two–way nested grids having resolution of 1, 3, 9, and 27 km were included in the simulation. It was initialized with conventional observational data, and a 30 h simulation and analysis of one sea–land breeze case were performed. It was shown that the model with a finer resolution (1 km) captures the sea breeze and land breeze in Macao with reasonable skill. The sea breeze front and the thermal internal boundary layer (TIBL) were also obviously revealed. However, the coarser horizontal resolution (3 km) could capture the sea breeze but not the land breeze.

Key words: Sea–land breeze, Simulation, Resolution

1. Introduction

The sea–land breeze circulation is still a subject of many articles found in the meteorological literature. It is a mesoscale phenomenon driven by diurnal heating and cooling contrasts between land and water. Thermal gradients caused by temperature differences between land and sea create onshore flow during the day (sea breeze) and offshore flow at night (land breeze). Atkinson (1981) compiled a brief review of the research about it. Simpson (1994) provided a detailed description of the physics and characteristics of its circulation.

The sea–land breeze has been investigated extensively with numerical models (e.g., Pielke, 1974; Arritt, 1993; Dailey and Fovell, 1999). Recently, the sea–land breeze system associated with the Pearl River estuary has been studied (Zhang et al., 1999). The Pearl River estuary consists of complex land–sea interface and terrain which makes the circulation more complicated over this area. In this paper we focused on the simulations of the sea–land breeze circulation in Macao, i.e., in the western part of the Pearl River estuary.

①This research is jointly supported by the grant of the Chinese State Commission of Science and Technology Climbing A "SCSMEX" and the National Natural Science Foundation of China (Grant No. 49794030).

This paper is organized as follows. Section 2 contains a brief model description and detailed configuration as well as its initialization. Section 3 presents results of the simulation. Finally, section 4 provides a brief summary.

2. Model description and initialization

The Penn State–National Center for Atmospheric Research (PSU–NCAR) MM5 in nonhydrostatic mode was used to simulate the sea–land breeze circulation in Macao and to provide additional data for diagnosing the three–dimensional flow around the Pearl River estuary. Grell et al. (1994) have given a detailed description of the MM5 and its capabilities, here only a brief summary is presented.

The simulation used the explicit moisture scheme of simple ice phase, and the cumulus parameterization of removing all available buoyant energy was applied except for the inner domain where the precipitation was explicitly resolved. The planetary boundary layer (PBL) was parameterized using the scheme of Zhang and Anthes (1982). The surface energy budget was used to calculate the ground temperature, and the sea surface temperature remained unchanged. Multilayer soil thermal diffusion was used. The long–wave and shortwave schemes were used for the radiation scheme with the radiation effects due to clouds. The radiation was computed every 30 minutes. In order to prevent gravity waves from being reflected off the model top, the upper radiative boundary condition was applied.

For this simulation, stationary 1, 3 and 9 km domains were nested within a 27 km domain using two–way nested grids. The center of the simulation domain is located at 23°N and 113°E. Four domains consist of, 84 × 84 grid points at 27 km domain (D01), 58 × 58 grid

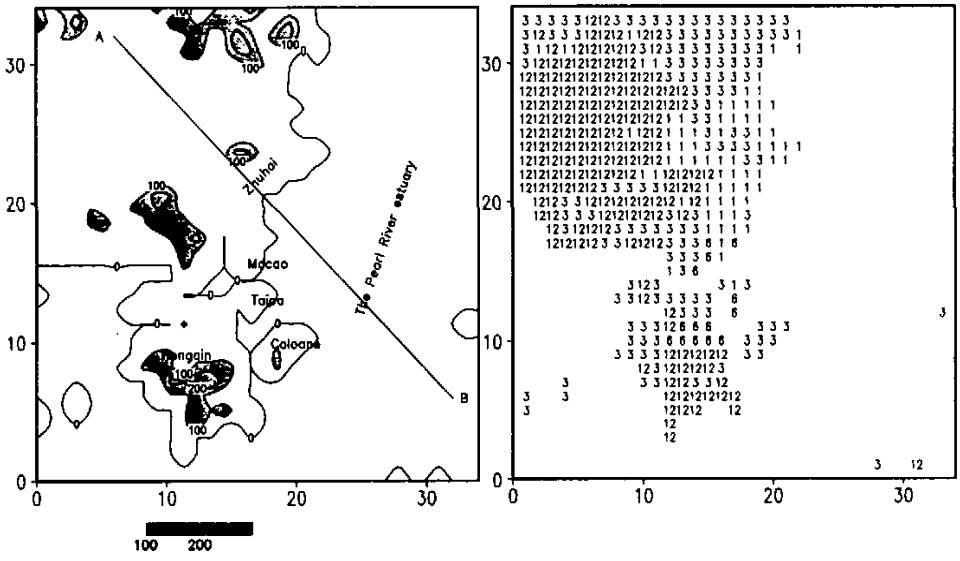

Fig. 1. (a) Model terrain height (m). (b) Landuse indices for the 1 km domain (D04). (The shaded area indicates that terrain height is larger than 100 m). (The landuse index 1 is for urban land, 3 for range–grassland, 6 for mixed forest and wet land, 12 for tropical or subtropical forest, and the blank areas for water body). The intervals between tick marks around the frames represent the number of grids in (a) and (b).

points at 9 km domain (D02), 34 × 34 grid points at 3 km domain (D03), and 34 × 34 grid points at 1 km domain (D04), respectively. Ten-minute averaged terrain data and five-minute averaged terrain data (PSU / NCAR) were interpolated to the 27 and 9 km model grids using a Cressman type objective analysis scheme and filtered by a two-pass smoother / desmoother, individually. For the 3 km domain, a 30 arc second global topography dataset (data source from Defence Mapping Agency) was interpolated to the grid in order to better resolve the Pearl River delta. The terrain dataset and the modified vegetation dataset of 1 km resolution same as Lin et al. (1998) were used to create the landuse of 3 km and 1 km domain. Figures 1a and 1b show the terrain and landuse of the D04. Twenty-three unevenly spaced full-sigma levels were used in the vertical profile. The 23 full-sigma levels were σ = 1, 0.99, 0.98, 0.96, 0.93, 0.89, 0.85, 0.80, 0.75, 0.70, 0.65, 0.60, 0.55, 0.50, 0.45, 0.40, 0.35, 0.30, 0.25, 0.20, 0.15, 0.10, 0.05, and 0.00 from surface to top respectively. The model top was considered to be at 100 hPa. The time step was 60 seconds for the coarse domain.

The 6-hourly data of global analyses (2.5° latitude-longitude resolution) of National Center for Environmental Predition (NCEP) were interpolated to the model grid data to serve as the first-guess fields. Surface and upper-air conventional observational data, which obtained from South China Sea Monsoon Experiment (SCSMEX) and Huaihe River Basin Energy and Water Cycle Experiment (HUBEX) dataset, were incorporated into the analysis using a Cressman-type analysis scheme. After the analyzed three-dimensional fields were produced, these grid data were interpolated to the 23 model sigma levels, and the integrated mean divergence in a column was removed to reduce error growth in the model simulation. The grid analyses were subsequently linearly interpolated in time to provide the lateral boundary conditions for 27 km domain. The model was initialized at 2000 local solar time (LST) 27 May 1998 (1200 UTC) with data from conventional observations and covers a 30 h period.

3. Case simulation and results

3.1 *Synoptic conditions*

At 2000 LST 27 May 1998, the 5880 m geo-potential height contour at 500 hPa, which was used to identify the periphery of the western Pacific subtropical high (WPSH), extended to the coast of southern South China Sea. At the surface, the wind flow was small around the Pearl River estuary. By 2000 LST 28 May 1998, although the WPSH shifted southward from 23°N to about 19°N, the wind flow at the surface was still small around the Pearl River estuary. This kind of synoptic case lacks strong synoptic-scale system over the southern South China Sea and the sea-land breeze circulation over the Pearl River estuary is easy to form.

To validate the model simulation for this case, we compared the observations of 850 hPa heights and wind fields with the simulation at 2000 LST 28 May 1998. The results show that the height field of the simulation matches quite well with the observations. The cyclonic flow around Taiwan, the westerly over the southern South China Sea and Vietnam and the anticyclone flow over the central China of the simulation were also consistent with the observations. However, a cyclonic flow appeared in the Guangxi province and the eastern Yunnan province on the simulation, but not existing in the observations (not shown).

3.2 *The surface flow field*

Fig. 2 shows partly near-surface winds (σ = 0.995) for the 1 km domain at 02:00, 04:00, 10:00, 12:00 and 16:00 LST 28 May, and 02:00 LST, 29 May.The simulation began at 2000 LST 27 May 1998. Before 0000 LST 28 May, southerly flow prevailed in Macao, Taipa and

Coloane. At 0200 LST 28 May, the northwesterly flow impinging on Zhuhai city had increased during the prior 4 hour, but the flow veered to southerly flow in 8 km southeastern outer region of the coast of Zhuhai city, in which a wind convergence zone exists (Fig. 2a). It could be recognized as the offshore distance of the offshore flow. At this time, however, the wind speed was still small in Macao and Taipa. At 0400 LST 28 May, the convergence zone was located about 8 km to the southeast of Coloane, and the northwesterly flow prevailed in Macao, Taipa, and Coloane (Fig. 2b). From 0600 to 0800 LST 28 May, subsequent solar heating of the land surface makes the marine air relatively more dense, but it takes time to overcome the offshore mean winds flow inland. Therefore, the remnants of the previous night's land breeze circulation persisted offshore and weakened slowly during this period (figures not shown). At 1000 LST 28 May, there was an onshore flow in the sea and an offshore flow in the land. Astonishingly, there existed a convergence zone associated with the sea breeze right along the eastern coast of Zhuhai although the sea–land interface is irregular (Fig. 2c). At the same time wind speed at Macao, Taipa and Coloane was small. But at 1200 LST 28 May, the modest south–southeasterly flow prevailed over Coloane and the southeasterly flow in Taipa and Macao (Fig. 2d). The convergence zone is located at about 9 km inland to the eastern coast of Zhuhai, i.e., the sea breeze has penetrated about 9 km inland. Meanwhile, the valley–wind prevailed over Hengqin Island because of mountain. Then the southeasterly on–shore flow around Macao, Taipa and Coloane was intensified and maintained. At 1600 LST 28 May, two sea breeze systems formed (Fig. 2e). In the eastern part of Zhuhai city and Macao, the flow was from the south–southeast with speeds of the order of about 6–7 m s^{-1}. In the western part of Hengqin Island, the flow was generally from the south, corresponding to another sea breeze system. The wind speeds were of the order of 5–7 m s^{-1}. Afterwards, the two sea breeze systems weakened gradually and slowly (figures not shown). At 0200 LST 29 May, the northwesterly flow prevailed around Zhuhai and Macao, the weak northerly flow in Taipa and Coloane (Fig. 2f). These results were found in agreement with diagnostic study of Zhang et al. (1999) for the sea breeze system of the Pearl River estuary.

3.3 *Vertical structure and PBL*

The simulated wind profiles at Taipa are shown in Fig. 3. The upper winds were the persistent westerlies during all the simulated periods. However, in the lower levels, the sea–land breeze changes were obvious along with time. Before 0000 LST May 28, the lower winds were the weak southerly winds. From 0200 LST to 0800 LST May 28, the lower offshore flows (northwesterly) prevailed. From 1000 LST to 2200 LST May 28, the lower onshore flows (southeasterly) was dominant. After 0000 LST May 29, the lower offshore flows could be seen. Thus, the rsults showed that the model captured the sea–land breeze with reasonable accuracy.

At 0400 LST 28 May, because of the strong radiational cooling of land at night, the stable PBL heights in land were smaller than 70 m (Fig. 4a). The PBL heights on the area that was effected by land breeze (offshore flow) were also small (70 to 200 m). The PBL heights in the sea away from the offshore distance of the offshore flow were about 300 m.

At 1200 LST 28 May, in the regions that were effected by the sea breeze, the PBL heights were smaller than 500 m. However, the PBL became mixed layer on land during daytime and its PBL heights were larger than 1000 m in other regions (Fig. 4b).

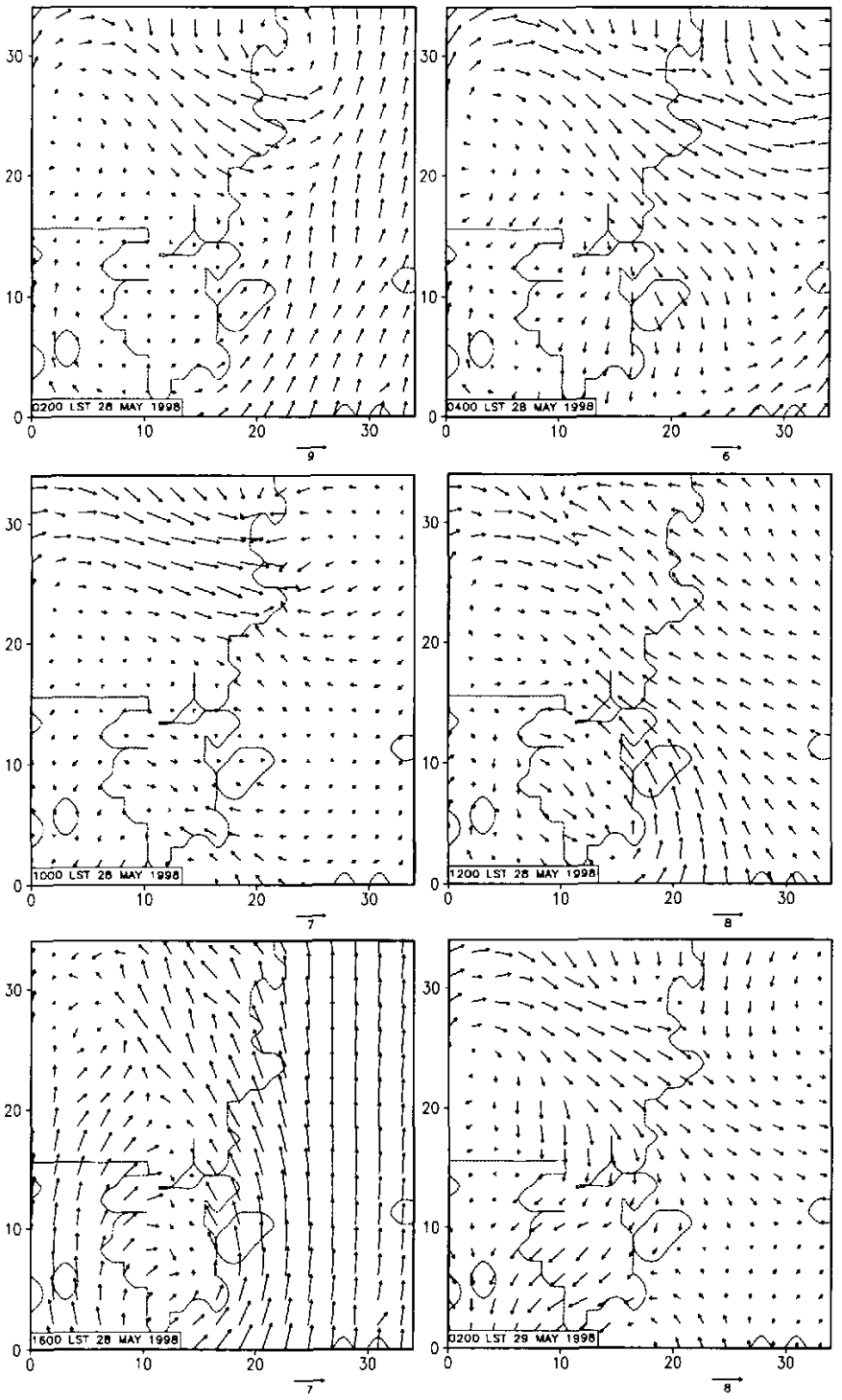

Fig. 2. The near-surface wind fields (σ = 0.995) for the simulation at (a) 0200 LST 28 May, (b) 0400 LST 28 May, (c) 1000 LST 28 May, (d) 1200 LST 28 May, (e) 1600 LST 28 May, and (f) 0200 LST 29 May, 1998. The dashed line in (a) indicates sea-land interface.

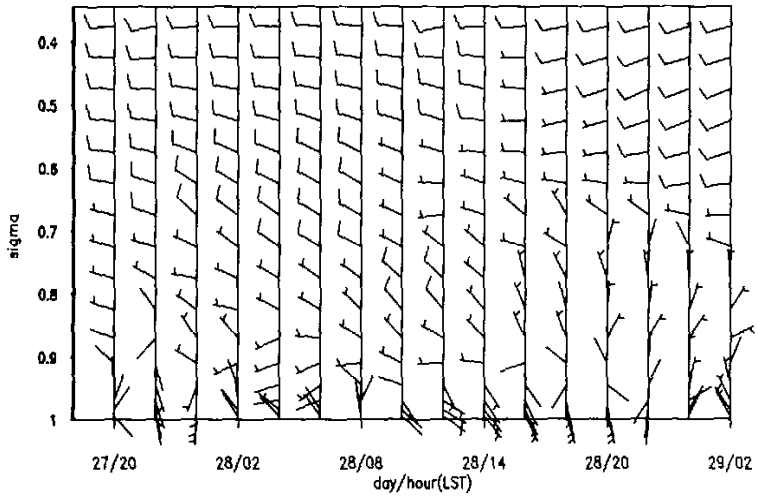

Fig. 3. The horizontal wind speed and direction displayed as time–sigma section of model between 2000 LST 27 May and 0200 LST May 29, 1998 simulated winds interpolated to Taipa. (A full wind barb represents 10 m / s).

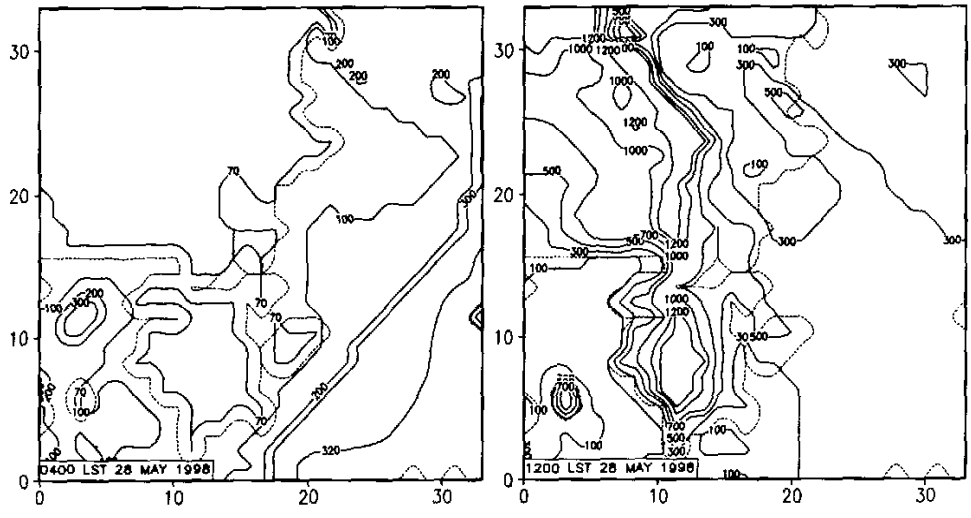

Fig. 4. The PBL heights according to Zhang and Anthes (1982) for the simulation at (a) 0400 LST 28 May, and (b) 1200 LST 28 May, 1998. The dashed line indicates sea–land interface.

At 0400 LST 28 May, the offshore flow (northwesterly flow) appeared in the western part of the Pearl River estuary. The depth of the simulated land–breeze layer was about between 100 m and 200 m (Fig. 5a). The horizontal speed of land breeze reached a maximum strength of 4.0 m s^{-1}. In the region of the strongest land breeze, the stratification was very stable, because the large–scale upper flow was a strong offshore flow, and the return flow was difficult

to distinguish.

By 1200 LST, 28 May, the sea-breeze horizontal flow was intensified. The horizontal speed of sea breeze reached 4.0 m s^{-1}, the maximal vertical motion reached 2.2 m s^{-1}(Fig. 5b). The sea-breeze front, which is defined by the location of zero ground-relative cross-shore flow or close proximity to the front's thermodynamic boundary (Dailey and Fovell, 1999), was formed. The front propagated almost 9 km inland and it was propagating at 5 km h^{-1} (see Fig.2d). The depth of the sea-breeze layer was about 700 m. The maximum vertical motion was located at the forward flank of the circulation above the sea-breeze front though the strongest onshore flow is still confined to the coast (Fig. 2d, 5b). The horizontal divergence also located at the Pearl River estuary. Both the frontal forced updraft and the seaward subsidence continued to intensify and expand. On the landward side of the sea-breeze front, the isentropes were raised at the top of the boundary. Behind the sea-breeze front, in the region of the strongest subsidence, the opposite was the case. This simulation was also somewhat analogous to Arritt's (1993) " moderate opposing flow" regime, which produced the strongest lifting along the sea breeze front.

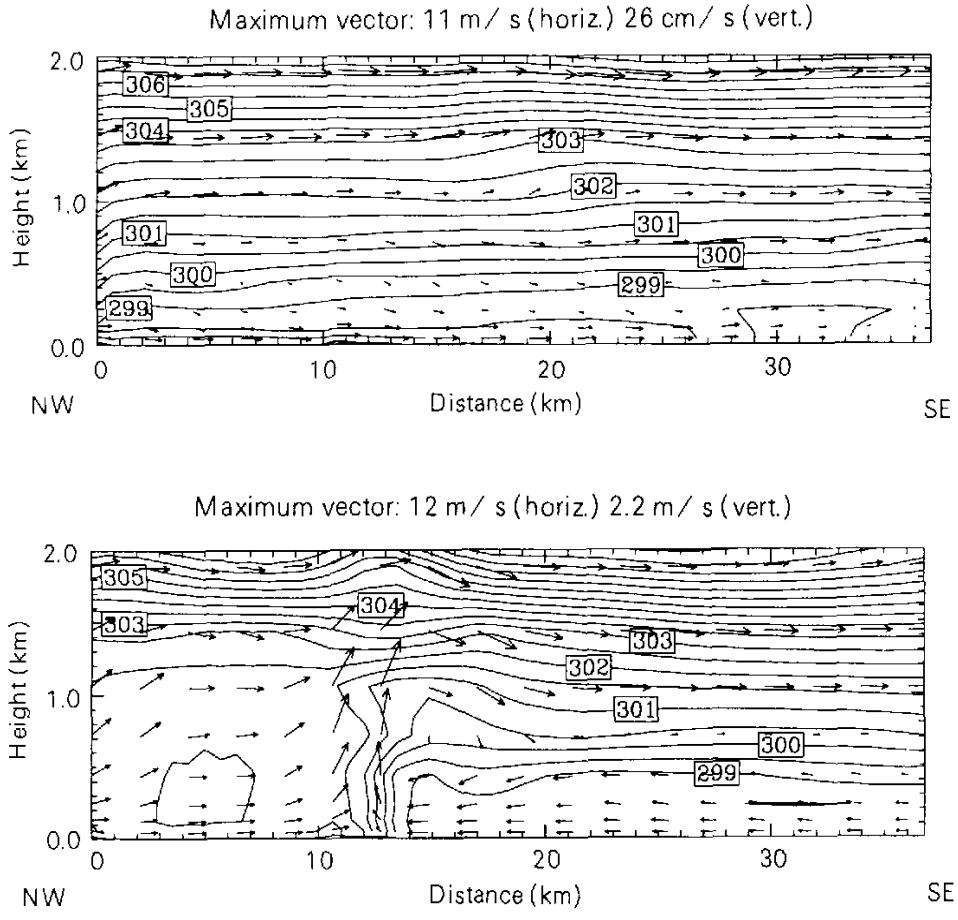

Fig. 5. Vertical cross section of the simulated potential temperature (at interval 0.5 K) and the winds along line AB in Figure 1(a) at (a) 0400 LST May 28, and at (b) 1200 LST May 28, 1998.

As the dynamical and thermal characteristics of the surface landuse between sea and land were different when the sea breeze penetrated inland, the thermal internal boundary layer (TIBL) formed. TIBL plays an important role in the transportation and diffusion of airborne material near coastline because the sea breeze fumigation occurs frequently from tall stacks at coastal locations. When the sea breeze prevailed at 1400 LST May 28, the TIBL obviously revealed in the simulation (Fig. 6). The TIBL depth ranged between 50 and 140 m, which is defined according to the turning of the isentrope cross-section in Fig. 6. It is shown that the TIBL depth in Fig. 6 does not agree with the square root law of the Weisman's (1976) formulation for defining the TIBL in sea breeze flows.

3.4 *Importance of horizontal resolution*

To test the importance of horizontal resolution for capturing this type of local circulation, we also performed a sensitivity experiment, in which domain 4 was removed, leaving 3 km as the finest resolution. The land breeze in the west of the Pearl River estuary was absent in the 3 km simulation (Fig. 7), and only the sea breeze was captured (figures not shown). The local mountain-valley circulation that located at Hengqin Mountain was also missing in the 3 km simulation. It is indicated that the coarse depiction of the terrain does not capture much of the local flows.

4. Summary

In this study, the new-generation operational mesoscale model, MM5, was used to study the sea-land breeze in the western part of the Pearl River estuary. The synoptic case lacking strong synoptic-scale system over the southern South China Sea is chosen because the sea-land breeze circulation over the Pearl River estuary was easy to commence in the situation.

A fourfold-nested simulation with a minimum horizontal grid size of 1-km captured the evolution and structure of the sea-land breeze over the Pearl River estuary. At the latter half of the night, the lower offshore flows (northwesterly) prevailed. Around midmorning and afternoon, however, the lower onshore flows (southeasterly) dominated. The results also

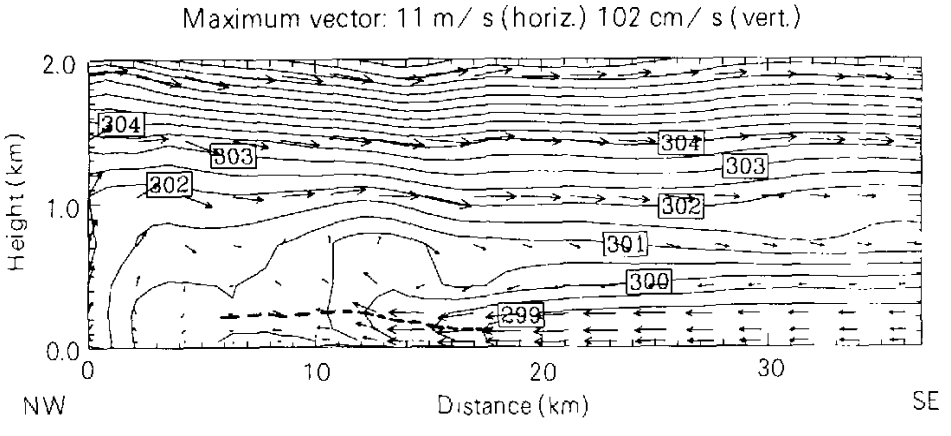

Fig. 6. As in Fig.5 but at 1400 LST May 28, 1998. TIBL is also shown as thick dashed line.

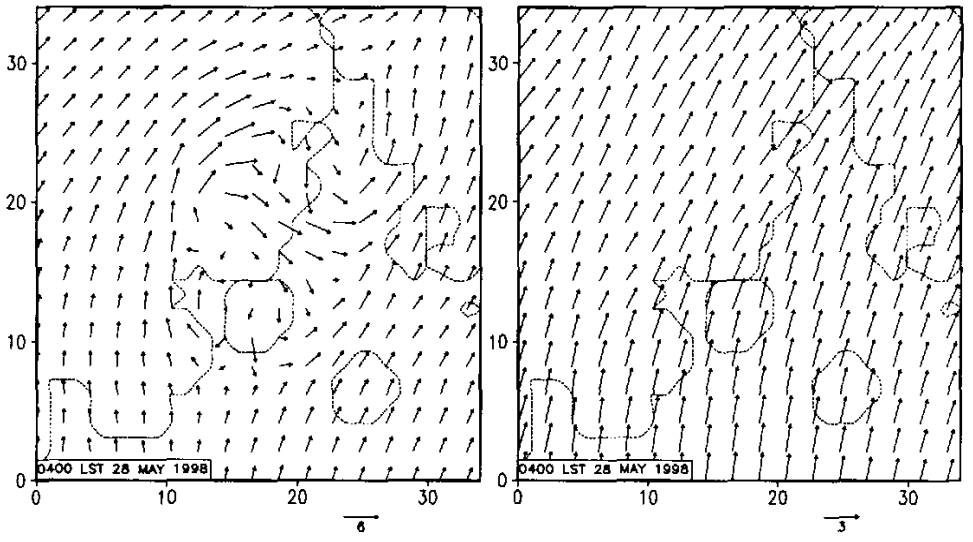

Fig. 7. The near-surface wind fields (σ =0.995) in domain 3 for the simulation at 0400 LST 28 May, 1998 for the experiment in which domain 4 (a) was removed, and (b) was included. The dashed line indicates sea-land interface.

showed that the model captured the sea breeze front and TIBL with reasonable skill. Meanwhile, sensitivity test suggested that the resolution of the model played an important role in the evolution of the near-surface land breeze.

The results of this study indicated a promising future for the simulation of fine-scale structures associated with topographically forced flows in the complex coastal zone. As demonstrated in this study, sophisticated nonhydrostatic models, such as MM5, are capable of simulating and predicting these complex local flows (for example, sea-land breeze) in an operational environment. Future studies will be greatly benefited if the detailed data is collected through special field program.

REFERENCES

Arritt, R. W., 1993: Effects of the large-scale flow on characteristic features of the sea breeze. *J. Appl. Meteor.*, **32**, 116-125.

Atkinson, B. W., 1981: *Meso-Scale Atmospheric Circulation*, London: Academic Press, 495pp.

Benjamin, S. G., and N. L. Seaman, 1985: A simple scheme for objective analysis in curved flow. *Mon. Wea. Rev.*, **113**, 1184-1198.

Chen Jiang, Chen Yuneng, and Chen Wanlong, 1993: A numerical study on the two-dimensional sea and land breezes. *Chinese Journal of Atmospheric Sciences*, **17(3)**, 359-368 (in Chinese).

Dailey, P. S., and R. G. Fovell, 1999: Numerical simulation of the interaction between the sea-breeze front and horizontal convective rolls. Part I: Offshore ambient flow. *Mon. Wea. Rev.*, **127**, 858-878.

Grell, G. A., J. Dudhia, and D. R. Stauffer, 1994: *A Description of the Fifth-Generation Penn State/ NCAR Mesoscale Model (MM5)*. NCAR Tech. Note NCAR / TN-398+STR, 138pp.

Lin Wenshi, Fan Shaojia, Zhu Wei, Liu Liming, Xiao Wanneng, and Pan Rongqing, 1998: Meteorological comprehension of high resolution land classification over the gate of the Pearl River and its neighborhood. *Journal of*

Zhongshan University, **37(Suppl. 2)**, 144–147 (in Chinese).

Pielke, R. A., 1974: A three-dimensional numerical model of the sea breezes over south Florida. *Mon. Wea. Rev.*, **102**, 115–139.

Simpson, J. E., 1994: *Sea Breeze and Local Wind*, New York, Cambridge University Press, 234pp.

Weisman, B., 1976: On the criteria for the occurrence of fumigation inland from a large lake. *Atmos. Environ.*, **10**, 172–173.

Zhang, D., and R. A. Anthes, 1982: A high-resolution model of the planetary boundary layer—Sensitivity test and comparisons with SESAME-79 data. *J. Appl. Meteor.*, **21**, 1594–1609.

Zhang Lifeng, Zhang Ming, and P. Lam, 1999: Study of sea-land breeze system in the mouth area of the Zhujiang River. *Chinese Journal of Atmospheric Sciences*, **23(5)**, 581–589 (in Chinese).

澳门及其邻近地区海陆风的模拟

林文实　王安宇　吴池胜

冯瑞权　古志明

摘　要

利用宾州／美国国家大气研究中心的 MM5 模式来模拟澳门的海陆风和珠江口的三维风场。模式设计为四重套网格，分辨率分别为 1 km, 3 km, 9 km, 27 km。使用常规观测资料作为初始场，模拟时间为 30 小时。结果表明采用高分辨率(1 km)模拟能很好地捕捉到澳门的海风和陆风。海风锋和热力内边界层也清楚可见。如果最小分辨率为 3 km，则只捕捉到海风、陆风却模拟不出来。

关键词：海陆风，模拟，分辨率